TEXAS
The University of Texas at Austin

Staged Strategy to Avoid Hospital Surge and Preventable Mortality, while Reducing the Economic Burden of Social Distancing Measures

Haoxiang Yang, Daniel Duque, Özge Sürer, David P. Morton,
Remy Pasco, Kelly Pierce, Spencer J. Fox, Lauren Ancel Meyers

The University of Texas at Austin
COVID-19 Modeling Consortium

utpandemics@austin.utexas.edu

Staged Strategy to Avoid Hospital Surge and Preventable Mortality, while Reducing the Economic Burden of Social Distancing Measures

Presented to the city of Houston on June 15, 2020

The University of Texas COVID-19 Modeling Consortium

Contributors: Haoxiang Yang, Daniel Duque, Özge Sürer, David P. Morton, Remy Pasco, Kelly Pierce, Spencer J. Fox, Lauren Ancel Meyers

Contact: utpandemics@austin.utexas.edu

Background

In order to balance the goals of preventing death from COVID-19 while also minimizing other negative (societal and economic) impacts, it is important to have a clear monitoring strategy that can guide public policy. Such a strategy can be used to help guide application of the range of non-pharmacological interventions that have been shown to reduce disease transmission and death. Here, we propose a coherent data-driven strategy for triggering both the tightening and relaxing of policies to ensure COVID-19 hospitalizations do not exceed healthcare capacity in the nine-county Houston Metropolitan Statistical Area (MSA) while minimizing the duration of restrictions on commerce, healthcare, recreation, and schooling.

As Texas and other US states reopen during the COVID-19 pandemic, it is expected that cases will increase. The goal of this strategy is to reduce economic hardship while maintaining access to hospital care for both COVID-19 patients and all other patients, and to avoid excess serious complications or death for those with COVID-19 or for those with other medical conditions like cancer or cardiovascular disease, who may not receive timely or safe care if the health system is overwhelmed by COVID-19. In addition, an overwhelmed health system creates a more dangerous environment for our health care providers who will be more likely to be infected and hence exacerbate health care shortages. Overwhelming the system could also seriously compromise the public's confidence in their health and safety.

To support planning by the city of Houston and Harris County, we built a model of COVID-19 transmission through the Houston MSA with a population of 6.9 million people. The model projects hospitalizations under different social distancing scenarios. Using this model, we derive a framework to support Houston area decision-makers in tracking the changing levels of COVID-19 risk and deciding when to reinstate and relax social distancing and other mitigation measures. We are providing these recommendations prior to peer review to provide intuition for both policy makers and the public regarding the evolving threat of COVID-19 and the judicious use of social distancing measures to slow spread and manage the risk of hospital surges.

Note that the results presented herein are based on multiple assumptions about the transmission rate and age-specific severity of COVID-19. Key aspects of the transmission dynamics of this virus are still uncertain, including the extent of asymptomatic infection and transmission. Our trigger recommendations are based on plausible scenarios for COVID-19 transmission in the Houston area and will require regular updating as our understanding of the virus and the state of the pandemic in Houston evolves.

Thresholds

Policy makers have proposed to track several data streams throughout the COVID-19 pandemic and initiate reopening policies when specific epidemiological thresholds are achieved, including: flu-like illness syndromic surveillance, case counts, deaths, test and trace metrics, and hospital capacity; see Table A in the Appendix. The reliability and timeliness of each of these sources has been variable across time and jurisdiction. Until COVID-19 testing capacity and priorities stabilize, COVID-19 hospital admissions will likely provide the best balance of accuracy and timeliness for determining when to pause, brake, or accelerate reopening policies.

Proposed Strategy

Given the goal of preventing a hospital surge that overwhelms the health system leading to excess death, the daily new COVID-19 hospital admissions (7-day rolling average) is a reliable indicator of the pace of pandemic transmission and can be used to trigger the reinstatement and relaxation of social distancing and other COVID-19 mitigation policies.

COVID-19 hospital admissions can be used to gauge the speed of COVID-19 transmission and project the future trajectory of pandemic waves in a community. Through modeling, we can determine “triggers” for when a surge is coming, which would indicate the need for a stricter social distancing guideline, or even a

shelter-in-place order. We can adjust staged reopening plans based on clear thresholds in daily hospital admissions to avoid reaching a point where a full-blown stay-home measure is “triggered.” This strategy complements other efforts to mitigate the pandemic, including wearing of face masks, and increasing testing and tracing, as these are essential to driving down the transmission of the virus.

Two critical pieces of data are required to implement this strategy for a given metropolitan area or region:

1. Safe hospital capacity — the total number of COVID-19 patients that can be treated at one time across the metro/region.

2. Real-time COVID-19 hospitalization data — new, daily, confirmed, hospital admissions for individuals requiring care for COVID-19

Proposed Triggers for the Houston MSA

Analysis 1 – Projected healthcare demand under constant levels of social distancing

Based on Harris County's recent COVID-19 Threat Level System (https://www.readyharris.org/stay-safe), we analyze four different levels of mitigation through social distancing, testing/tracing/isolation and other precautionary measures, as shown in Table 1. For each level, we make assumptions regarding the impact of mitigation measures on the (i) transmission rate in low risk populations, (ii) the transmission rate in high risk populations (cocooning), and (iii) whether schools can open in the fall. The assumed values are based on estimates derived from COVID-19 hospitalization data for Houston's nine-county MSA between April 2, 2020 and May 22, 2020.

Table 1: Model inputs for the four Harris County COVID-19 Levels. For each level, we specify a reduction in the transmission rate for low risk and high risk populations, as well and whether schools can be open.

Levels and Descriptions		Transmission Reduction in Low Risk Groups	Transmission Reduction in High Risk Groups (Cocooning)	School Closed
Level 4	**Limited Social Distancing**	**0.468**	**0.668**	**No**
Level 3	**Stay Vigilant**	**0.601**	**0.734**	**No**
Level 2	**Minimize All Contacts**	**0.706**	**0.734**	**No**
Level 1	**Stay Home**	**0.734**	**0.734**	**Yes**

Figure 1 projects the number of hospitalizations we would expect in the Houston MSA through summer of 2021 assuming that Houston remains in each one of the levels given in Table 1. The top left plot assumes that Houston's stay home order enforced Level 1 (red) social distancing between March 18, 2020 and May 22, 2020, and, afterwards, the population relaxed to the lightest Level 4 (blue) degree of social distancing. The other three plots are similar, with the other three levels of social distancing achieved after May

22. The horizontal lines correspond to three scenarios for COVID-19 hospital surge capacity in the Houston MSA, as provided by city officials: 4,500, 9,000 or 13,500 beds.

The insets provide a magnified comparison between the projected hospitalization numbers and the reported hospitalization counts across the MSA (red points) through June 10, 2020. The observed data most closely match the projections under the lightest (Level 4) restrictions from May 22, 2020 and June 10, 2020. If Houston has indeed rebounded to double the transmission rate relative to the April stay-home period (blue), then we would expect a COVID-19 hospitalization surge that picks up in late June grossly exceeds the largest possible hospital capacity, 13,500 beds, by the fall of 2020, unless stricter measures are enacted.

If the COVID-19 hospital surge capacity is 4,500 beds, then we would expect the pandemic to exceed capacity in all scenarios except an indefinite Level 1 (stay-home) order. However, an extended Level 1 order is likely untenable given numerous economic, political, and psychosocial factors.

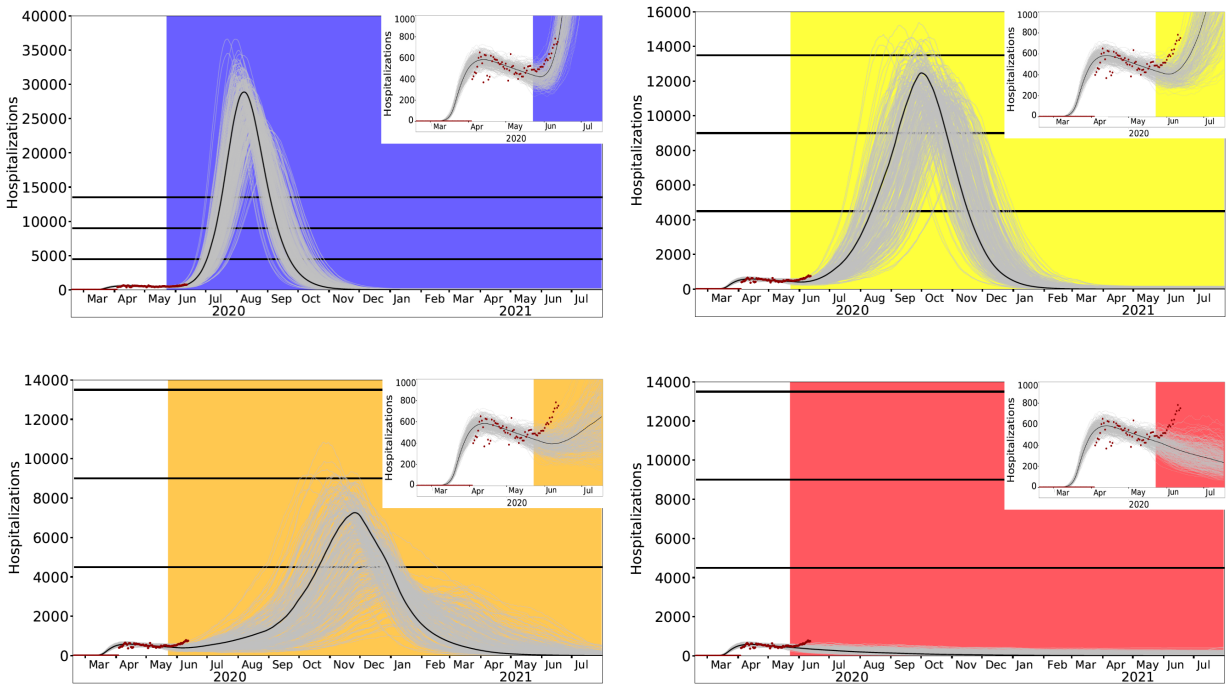

Figure 1. Projected COVID-19 hospitalizations in the Houston MSA assuming social distancing remains at a fixed level starting May 22, 2020. Background colors correspond to the Harris County COVID:19 levels: top left – Level 4; top right – Level 3; bottom left – Level 2; bottom right – Level 1. The black curves show the deterministic projections, the light gray curves indicate 300 stochastic simulations, and the red points indicate the reported COVID-19 hospitalizations through June 10, 2020. The insets magnify the first 150 days of the projection. The horizontal lines indicate three different COVID-19 hospital surge capacities of 4500, 9000, and 13,500 beds.

Analysis 2 – Suggested Triggers for Moving Between Levels

As described in Analysis 1, a fixed single-level may not be suitable to contain the pandemic while minimizing negative impacts. A flexible strategy would allow multiple levels of reopening. Moving between levels (braking or accelerating) would be guided by the number of daily hospital COVID-19 admissions in a region to prevent both a "surge" with excess mortality and reduce the need for a full "stay-at-home" order.

We have derived triggers for the Houston MSA that are expected to prevent an overwhelming surge in hospitalizations while reducing the need for Level 1 and Level 2 restrictions (Table 2). Figure 2 projects COVID-19 hospitalizations under these triggers. The policy is expected to allow Houston to remain largely in Levels 2-4, and considerably reduce the need for stay-home (Level 1) orders. The projections assuming a COVID-19 hospital surge capacity of 4,500 indicate that Houston may be able to avoid requiring a Level 1 stay-home order, although the bulk of the July-December 2020 is in Level 2. If the capacity is 9,000 or 13,500 beds, then Houston can reduce, or even eliminate, the time spent in Level 2 restrictions.

Level and Descriptions		Triggers		
		Hospital Capacity		
		4500	9000	13500
Level 4	Limited Social Distancing	<50	<70	<80
Level 3	Stay Vigilant	50-170	70-450	80-1140
Level 2	Minimize All Contacts	170-380	450-780	1140-1180
Level 1	Stay Home	>380	>780	>1180

Table 2: Recommended triggers to move between levels based on daily COVID-19 hospitalizations (7-day rolling average). For example, if the hospital capacity is 4500 and daily admissions grow above 170 then we recommend moving to Level 2 (orange).

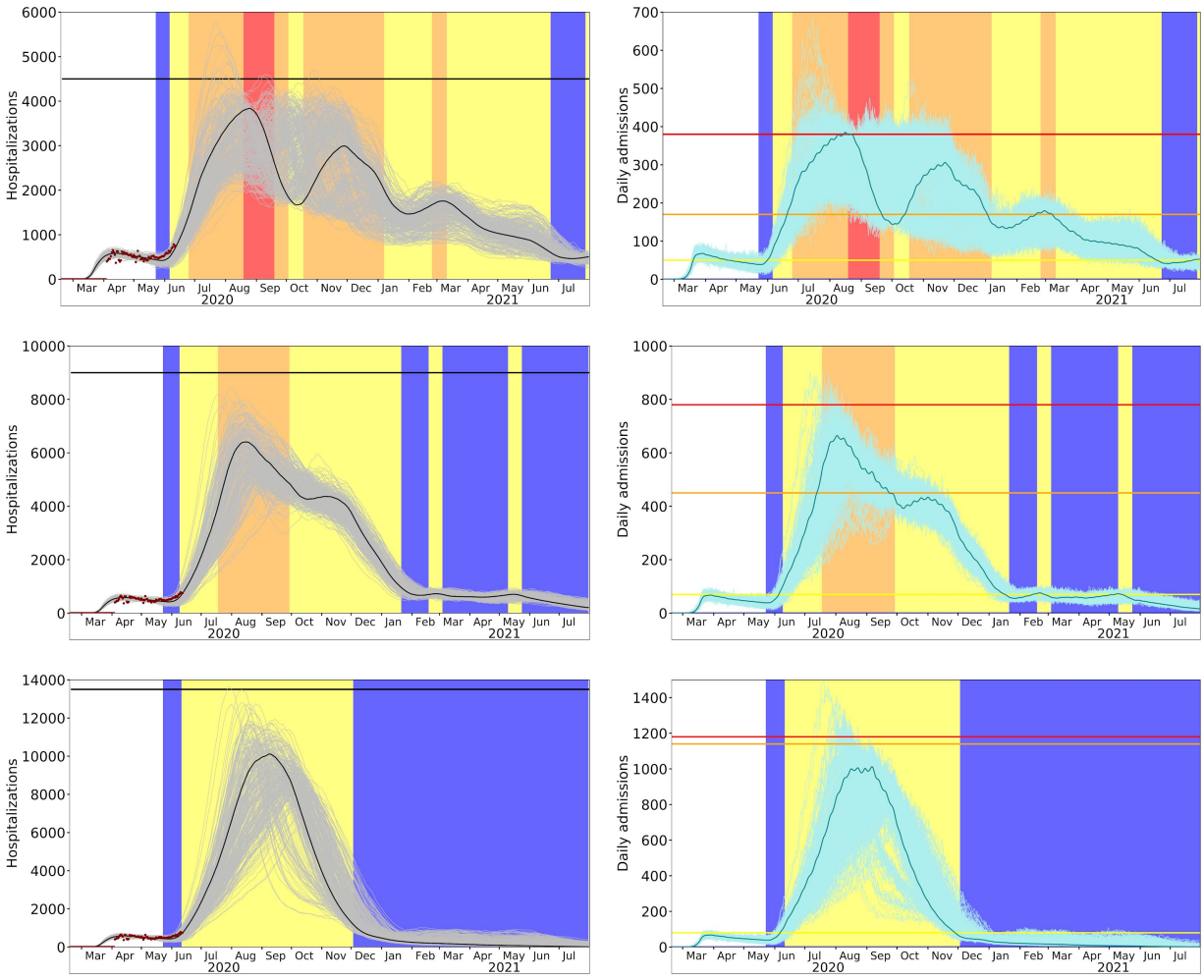

Figure 2. Projections for COVID-19 hospitalizations in the Houston MSA under optimized policies for reinstating and relaxing social distancing measures. The three rows correspond to three different COVID-19 surge capacities: 4,500, 9,000, and 13,500 beds, from top to bottom. Left-hand panels indicate daily hospitalizations (heads in beds). The solid black curves show the deterministic projection and gray paths indicate 300 stochastic simulations. Black horizontal lines indicate the assumed surge capacity; red points represent reported hospitalizations through early June 2020. Right-hand panels project the daily COVID-19 admissions (cyan) under the optimized strategies. The dark cyan curves show the deterministic projection and the light cyan lines indicate 300 stochastic simulations. The colored horizontal lines indicate the thresholds that trigger changes in risk levels: the (top) red lines are thresholds between Levels 1 and 2; the orange lines are thresholds between Levels 2 and 3; the yellow lines are thresholds between Levels 3 and 4. The policy goes down or up a level when the seven-day rolling average in daily admissions either surpasses or recedes below the corresponding threshold, respectively. In all panels, background colors indicate current COVID-19 restrictions (red, orange, yellow and blue correspond to Levels 1-4, respectively).

Communicating this strategy to the public could help create support to follow social distancing and reopening guidelines and allow businesses to anticipate changes in both opening and braking specific to their local community. If communities follow such social distancing guidance while increasing testing, tracing and isolation efforts to reduce transmission, they may never reach thresholds for full-fledged “lock-downs.”

Summary

New, daily, confirmed COVID-19 hospital admissions is an important measure to follow during reopening to prevent a hospital surge and excess deaths. It allows reliable estimates of local COVID-19 transmission rates and the determination of trigger/thresholds to allow a flexible and data-driven reopening plan. In the Houston MSA, the recommended thresholds can help to navigate the weeks and months ahead, but critically depend on the available hospital capacity for COVID-19 patients.

Appendix

Table A. Proposed measures for reinstating and relaxing social distancing measures.

Potential Measure	**Potential thresholds**	**Advantages**	**Disadvantages**	**Notes**
Influenza-like Illness (ILI) Syndromic Surveillance	Stable or Decreasing ILI for 2 weeks	May be earliest measure of increase cases	Many causes of ILI especially in fall/winter	Publicly reported data or COVID-19 symptom checker data
Case Count	Stable or Decreasing case counts for 2 weeks	Most closely reflects changes in infections; shortest lag between infection and reporting	Subject to bias based on changes in testing: capacity, priority populations, locations, reporting. Lags infections by at least 6+ days if primarily testing symptomatic cases.	Cases vary in risk of bad outcomes and transmission
Test Capacity	Daily per capita testing >0.1% population	Correlates with testing coverage that has achieved control in other countries	Higher prevalence will require more testing likely >0.15% population per day	
Test positivity rate	<5-10%	Allows for partial correction of changes in testing volume	Can be biased if testing is directed based on risk	Increase preoperative testing in very low risk group
Contact Tracing	>90% cases investigated >80% contacts traced	Finds new cases early and prevents spread	Lapses in quarantine or isolation threaten validity	Time dependent, ideally <48 hours
Hospital capacity	>20% Hospital & ICU beds available for surge	Closely tracks with risk of adverse outcomes	Difficult to define safe levels	Capacity can change quickly based on surgical volumes
COVID Deaths	Stable or decreasing deaths for 2 weeks	Easier to count	Attribution can be challenging; Lags other measures	

Total (excess) deaths	Return to baseline from historical controls	Easiest to count	Lags other measures; Hard to determine excess over expected	Assumes all excess due to COVID-19
New COVID-19 Admissions*	Trigger based on regional hospital capacity	Less subject to bias than case-based measures and total hospitalizations; Identifies important spectrum of disease	Lags infections by 10+ days; Harder to manage data	See Strategy Above

COVID-19 Epidemic Model Structure and Parameters

The model structure is diagrammed in Figure A1 and described in the equations below.
For each age and risk group, we build a separate set of compartments to model the transitions between the states: susceptible (S), exposed (E), pre-symptomatic infectious (P^Y), pre-asymptomatic infectious (P^A), symptomatic infectious (I^Y), asymptomatic infectious (I^A), symptomatic infectious that are hospitalized (I^H), recovered (R), and deceased (D). The symbols S, E, P^Y, P^A ,I^Y, I^A, I^H, R, and D denote the number of people in that state in the given age/risk group and the total size of the age/risk group is

$$N = S + E + P^Y + P^A + I^Y + I^A + I^H + R + D.$$

The model for individuals in age group a and risk group r is given by:

$$\frac{dS_{a,r}}{dt} = -S_{a,r} \cdot \sum_{i \in A} \sum_{j \in K} (I^Y_{i,j}\omega^Y + I^A_{i,j}\omega^A + P^Y_{i,j}\omega^{PY} + P^A_{i,j}\omega^{PA})\beta\phi_{a,i}/N_i$$

$$\frac{dE_{a,r}}{dt} = S_{a,r} \cdot \sum_{i \in A} \sum_{j \in K} (I^Y_{i,j}\omega^Y + I^A_{i,j}\omega^A + P^Y_{i,j}\omega^{PY} + P^A_{i,j}\omega^{PA})\beta\phi_{a,i}/N_i - \sigma E_{a,r}$$

$$\frac{dP^A_{a,r}}{dt} = (1-\tau)\sigma E_{a,r} - \rho^A P^A_{a,r}$$

$$\frac{dP^Y_{a,r}}{dt} = \tau\sigma E_{a,r} - \rho^Y P^Y_{a,r}$$

$$\frac{dI^A_{a,r}}{dt} = \rho^A P^A_{a,r} - \gamma^A I^A_{a,r}$$

$$\frac{dI^Y_{a,r}}{dt} = \rho^Y P^Y_{a,r} - (1-\pi)\gamma^Y I^Y_{a,r} - \pi\eta I^Y_{a,r}$$

$$\frac{dI^H_{a,r}}{dt} = \pi\eta I^Y_{a,r} - (1-\nu)\gamma^H I^H_{a,r} - \nu\mu I^H_{a,r}$$

$$\frac{dR_{a,r}}{dt} = \gamma^A I^A_{a,r} + (1-\pi)\gamma^Y I^Y_{a,r} + (1-\nu)\gamma^H I^H_{a,r}$$

$$\frac{dD_{a,r}}{dt} = \nu\mu I^H_{a,r}$$

where A and K are all possible age and risk groups, ^{A}, ^{Y}, ^{PA}, ω^{PY} are the relative infectiousness of the I^A, I^Y, I^{PA}, I^{PY} compartments, respectively, β is transmission rate, $_{a,i}$ is the mixing rate between age group a, $i \in A$, ^{A}, ^{Y}, ^{H} are the recovery rates for the I^A, I^Y, I^H compartments, respectively, σ is the exposed rate, ρ^A, ρ^Y are the pre-(a)symptomatic rates, τ is the symptomatic ratio, π is the proportion of symptomatic individuals requiring hospitalization, η is rate at which hospitalized cases enter the hospital following symptom onset, ν is mortality rate for hospitalized cases, and μ is rate at which terminal patients die.

We model stochastic transitions between compartments using the τ-leap method [1,2] with key parameters given in Tables A1-3. Assuming that the events at each time-step are independent and do not impact the underlying transition rates, the numbers of each type of event should follow Poisson distributions with means equal to the rate parameters. We thus simulate the model according to the following system of equations, henceforth called the *epidemic simulation equations*:

$$S_{a,r}(t+1) - S_{a,r}(t) = -P_1$$
$$E_{a,r}(t+1) - E_{a,r}(t) = P_1 - P_2$$
$$P^A_{a,r}(t+1) - P^A_{a,r}(t) = (1-\tau)P_2 - P_3$$
$$P^Y_{a,r}(t+1) - P^Y_{a,r}(t) = \tau P_2 - P_4$$
$$I^A_{a,r}(t+1) - I^A_{a,r}(t) = P_3 - P_5$$
$$I^Y_{a,r}(t+1) - I^Y_{a,r}(t) = P_4 - P_6 - P_7$$
$$I^H_{a,r}(t+1) - I^H_{a,r}(t) = P_7 - P_8 - P_9$$
$$R_{a,r}(t+1) - R_{a,r}(t) = P_5 + P_6 + P_8$$

with

$$P_1 \sim \text{Pois}(S_{a,r}(t)F_{a,r}(t))$$
$$P_2 \sim \text{Pois}(\sigma E_{a,r}(t))$$
$$P_3 \sim \text{Pois}(\rho^A P^A_{a,r}(t))$$
$$P_4 \sim \text{Pois}(\rho^Y P^Y_{a,r}(t))$$
$$P_5 \sim \text{Pois}(\gamma^A I^A_{a,r}(t))$$
$$P_6 \sim \text{Pois}((1-\pi)\gamma^Y I^Y_{a,r}(t))$$
$$P_7 \sim \text{Pois}(\pi\eta I^Y_{a,r}(t))$$

$$P_8 \sim \text{Pois}((1-\nu)\gamma^H I_a^H)$$
$$P_9 \sim \text{Pois}(\nu\mu I_{a,r}^H(t))$$

and where $F_{a,r}$ denotes the force of infection for individuals in age group a and risk group r and is given by:

$$F_{a,r}(t) = \sum_{i\in A}\sum_{j\in K}(I_{i,r}^Y(t)\omega^Y + I_{i,r}^A(t)\omega^A + P_{i,j}^Y(t)\omega^{PY} + P_{i,j}^A(t)\omega^{PA})\beta_{a,i}\phi_{a,i}/N_i$$

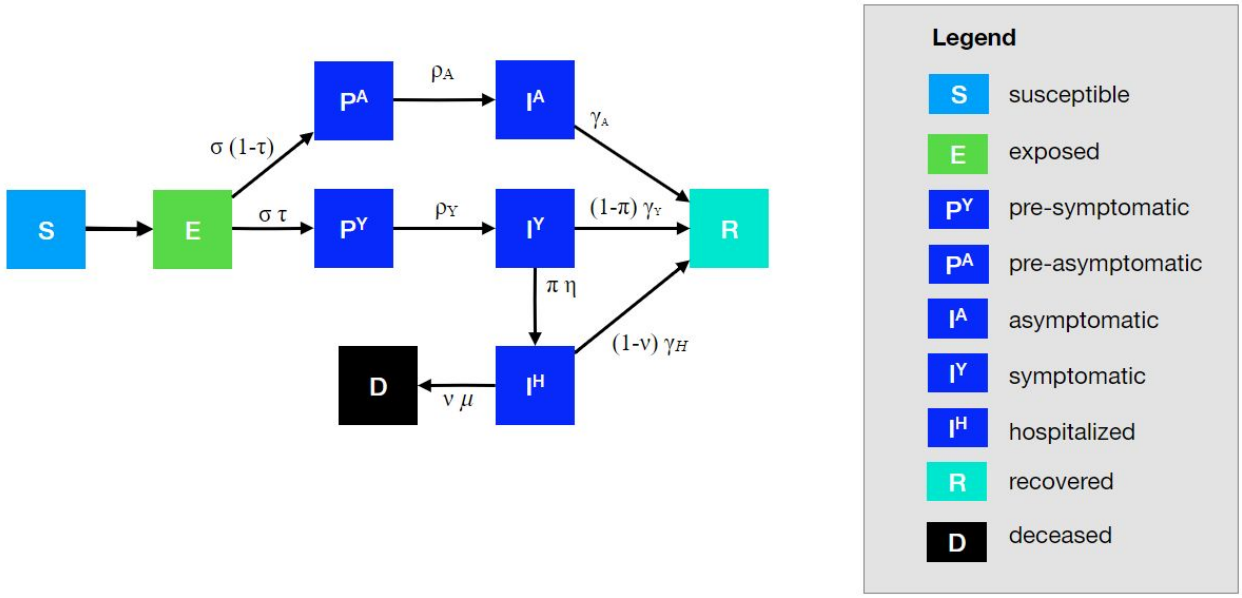

Figure A1. Compartmental model of COVID-19 transmission in a US city. Each subgroup (defined by age and risk) is modeled with a separate set of compartments. Upon infection, susceptible individuals (*S*) progress to exposed (*E*) and then to either pre-symptomatic infectious (P^Y) or pre-asymptomatic infectious (P^A) from which they move to symptomatic infectious (I^Y) and asymptomatic infectious (I^A) respectively. All asymptomatic cases eventually progress to a recovered class where they remain protected from future infection (*R*); symptomatic cases are either hospitalized (I^H) or recover. Mortality (*D*) varies by age group and risk group and is assumed to be preceded by hospitalization.

Trigger Threshold Selection Methods

We optimize the timing of when to initiate different levels of reopening, guided by triggers that monitor both daily new-hospital admissions and total hospitalizations. Triggering to a level corresponding to a tighter lockdown occurs when a seven-day moving average of daily hospital admissions grows to exceed an optimized threshold. Moving to a more relaxed level occurs when: (a) the same moving average drops below the level threshold and (b) total hospitalizations are under a safety threshold. Each level corresponds to a percentage of reduction in transmission, school closure, and a cocooning level for the high-risk population.

In addition to epidemiological constraints governing the transmission and severity of the virus, our optimization model selects triggers that ensure the aggregate daily arrival rate of new patients to hospitals is such that, with high probability, the demand for hospital beds does not exceed supply. We use the square-root staffing rule of [3] for an M/M/s queue. The parameter of this queue is set up to ensure a probability of over 0.99997 for a single arriving patient to have a bed when admitted. We assume that imposing level k is associated with a daily socioeconomic cost, c^k, and we propose an optimization model that seeks trigger thresholds to minimize the total cost to the model's horizon.

The optimization framework we use follows that in [4], with distinctions in the following three details:

1. *Higher fidelity simulation model:* In particular, we use the updated simulation model as shown in Figure A1, which adds pre-symptomatic and pre-asymptomatic compartments. Parameters are updated as well according to Table A1-A4. These equations correspond to the dynamical equations labeled Constraints (1) in Duque et al. [4], and here we name them "epidemic simulation constraints."

2. *Multiple levels versus single level*: In [4], we can toggle between two states using a threshold, which can adapt over time, as well as the hospitalization safety threshold. In the current multi-level model, we fix r to be 60% of the hospital capacity. Furthermore, we search for a set of level thresholds, l^k, where $k \in K$ indexes the levels for increasingly strident levels of risk reduction. Level k is executed when either of the following criteria are met. (These are similar to Constraints (2) in reference [4], and we name them "stage determination criteria."): (1) Increase (tighten) the level: The 7-day moving average of hospitalization admissions exceeds level k's threshold, and the current level $k-1$ has been executed for longer than the minimum length (i.e., 14 days in our implementation); (2) Decrease (relax) the level: The 7-day moving average of hospitalization admissions is smaller than the current level $k+1$'s threshold, the current hospitalization number is below safety threshold, r, and the current level $k+1$ has been executed for longer than the minimum length (14 days). We can define the indicator variables X_t^k as:

$$X_t^k = \begin{cases} 1 & \text{if stage } k \text{ is executed at time } t \\ 0 & \text{otherwise} \end{cases},$$

and the optimization model can be written as:

$$\min_{l^k} E_\omega \sum_{t\in\mathcal{T}} \sum_{k\in\mathcal{K}} c^k X_t^k \quad \text{s.t.} \quad \begin{array}{l} \{l^k\}_{k\in\mathcal{K}} \in \mathcal{F} \\ \text{the epidemic simulation equations} \\ \text{the stage determination criteria} \end{array}$$

The collection of feasible sets of thresholds, is defined as follows:

. $l^{|K|+1} = +\infty$

. $0 \leq l^k \leq l^{k+1} \quad \forall k \in K$

· With the sample path corresponding to a point forecast (i.e., model (3) in [4]), the daily hospitalizations obtained must satisfy the square-root staffing rule.

3. *Chance constraint and optimality criterion*: In reference [4], we consider the candidate set of thresholds feasible as long as a chance constraint is met, i.e., the probability that the number of "heads in beds" exceeds hospital capacity is below a specified level. Here, we revise our selection rules for an optimal set of thresholds as follows:

    a. First, among thresholds satisfying the chance constraint defined as inequality (4e) in reference [4], we select the one with the lowest expected cost;

    b. Second, if the chance constraint is infeasible we select thresholds with the smallest violation of the chance constraint. If there is a tie in the violation, we select a solution with the lowest expected cost.

Estimating Epidemic Start Date and Transmission Reduction Following Houston's Stay-Home Order

We estimated the COVID-19 epidemic start date and transmission rate reduction due to social distancing in the Houston MSA using least-squares fitting, which compares the predicted and observed numbers of daily hospitalizations (i.e., heads in beds) for the Houston MSA. We assume that transmission was reduced starting on March 18, 2020, based on a substantial change in mobility patterns reflected in cellular phone GPS movement data (Figure A2). Since we lacked sufficient *early* COVID-19 hospitalization data from Houston to estimate a baseline transmission rate (β), we assumed a value estimated from a more complete set of hospitalization data from the Austin-Round Rock MSA. We further assume that: (i) the epidemic starts with a single case, (ii) the transmission rate decreases by an amount d_1 on March 18th, and (iii) the transmission rate decreases when school closures are enacted on March 19, 2020 (by an amount determined by our pre-set contact matrices).

We estimate d_1 using a nonlinear least squares fitting procedure in the SciPy/Python package across a range of possible start dates [5]. For a given start date, we run a deterministic simulation of our model assuming a central value for d_1. Using a trust region method, the algorithm finds value of d_1 that minimize the sum of squared daily differences between the simulated ($\hat{H}_t$) and actual (H_t) daily hospitalizations from March 13 through April 19 2020: for the assumed start date as $S(d) = \sum_t \left(H_t = \hat{H}_t\right)^2$. We then select the simulation start date that produces the lowest normalized mean square deviation and fix that start date for subsequent simulations. For the Houston MSA, the best-fit simulation start date is February 19, 2020. The decreased contact is assumed to stay in effect until May 22, 2020.

Table A1. Initial conditions, school closures and social distancing policies

Variable	Settings
Initial day of simulation	2/19/2020
Initial infection number in locations	1 pre-symptomatic case in 18-49y age group
School closure	3/19/2020 - 8/24/2020. After 8/24/2020: scenario-specific or policy-specific
Age-specific and day-specific contact rates	Home, work, other and school matrices provided in Tables S4.1-S4.4, and are modified to reflect school closures and other changes in contact patterns and transmission rates during simulations

Table A2. Model parameters[a]

Parameters	Best guess values	Source
β: baseline transmission rate	0.0640	Fitted to daily COVID-19 hospitalizations in Houston MSA
κ: reduction in transmission	From 2020-02-27 to 2020-03-17: 0 From 2020-03-17 to 2020-05-22: 0.74 After 2020-05-22: Depends on the policy	From 2020-03-17 to 2020-05-22: fitted to daily COVID-19 hospitalizations in Houston MSA
γ^A: recovery rate on asymptomatic compartment	Equal to γ^Y	
γ^Y: recovery rate on symptomatic non-treated compartment	$\frac{1}{\gamma^Y} \sim Triangular(3.0, 4.0, 5.0)$	He et al. [6]
τ: symptomatic proportion	0.57	Gudbjartsson et al. [7]
σ: exposed rate	$\frac{1}{\sigma} \sim Triangular(1.9, 2.9, 3.9)$	Based on incubation [8] and pre-symptomatic periods
ρ^A: pre-asymptomatic rate	Equal to ρ^Y	
ρ^Y: pre-symptomatic rate	$\frac{1}{\rho^Y} = 2.3$	He et al. [6]
P: proportion of pre-symptomatic transmission (%)	44	He et al. [6]
ω^Y: relative infectiousness of symptomatic individuals	1.0	By construction

ω^P : relative infectiousness of pre-symptomatic individuals	$\omega^P = \frac{P}{1-P}\frac{\tau\omega^Y\left[YHR/\eta + (1-YHR)/\gamma^Y\right] + (1-\tau)\omega^A/\gamma}{\tau\omega^Y/\rho^Y + (1-\tau)\omega^A/\rho^A}$ $\omega^{PY} = \omega^P\omega^Y, \omega^{PA} = \omega^P\omega^A$	
ω^A: relative infectiousness of infectious individuals in compartment I^A	$\omega_A \sim Triangular(0.29, 0.29, 1.4)$	$\frac{1}{\omega_A}$:1.5 (95% CI: 0.7-3.4) from He et al. [9]
IFR: infected fatality ratio, age specific (%)	Low risk: [0.0009167, 0.002179, 0.03388, 0.2520, 0.6440] High risk:[0.009167, 0.02179, 0.3388, 2.520, 6.440]	Age adjusted from Verity et al. [10]
YFR: symptomatic fatality ratio, age specific (%)	Low risk: [0.001608, 0.003823, 0.05943, 0.4420, 1.130] High risk: [0.01608, 0.03823, 0.5943, 4.420, 11.30]	$YFR = \frac{IFR}{\tau}$
h: high-risk proportion, age specific (%)	[7.1315, 11.0361, 18.7665, 33.6906, 47.9775]	Estimated using 2015-2016 Behavioral Risk Factor Surveillance System (BRFSS) data with multilevel regression and poststratification using CDC's list of conditions that may increase the risk of serious complications from influenza[11–13]

[a]Values given as five-element vectors are age-stratified with values corresponding to 0-4, 5-17, 18-49, 50-64, 65+ year age groups, respectively.

Table A3 Hospitalization parameters

Parameters	Value	Source
γ^H: recovery rate in hospitalized compartment	$\frac{1}{\gamma^H} \sim Triangular(9.4, 10.7, 12.8)$	Fit to Austin admissions and discharge data (Avg=10.96. 95% CI = 9.37 to 12.76)
YHR: symptomatic case hospitalization rate (%)	Low risk: [0.04021, 0.03091, 1.903, 4.114, 4.879] High risk: [0.4021, 0.3091, 19.03, 41.14, 48.79]	Age adjusted from Verity et al. [10]
π: rate of symptomatic individuals go to hospital, age-specific	$\pi = \frac{\gamma^Y * YHR}{\eta + (\gamma^Y - \eta)YHR}$	
η: rate from symptom onset to hospitalized	0.1695	5.9 day average from symptom onset to hospital admission Tindale et al.[14]

μ: rate from hospitalized to death	$\frac{1}{\mu} \sim Triangular(5.2, 8.1, 10.1)$	Fit to Austin admissions and discharge data (Avg=7.8, 95% CI = 5.21 to 10.09)
HFR: hospitalized fatality ratio, age specific (%)	[4, 12.365, 3.122, 10.745, 23.158]	$HFR = \frac{YFR}{YHR}$
ν: death rate on hospitalized individuals, age specific	$\nu = \frac{\gamma^H HFR}{\mu + (\gamma^H - \mu)HFR}$	

Table A4.1 Home contact matrix. Daily number contacts by age group at home.

	0-4y	**5-17y**	**18-49y**	**50-64y**	**65y+**
0-4y	0.5	0.9	2.0	0.1	0.0
5-17y	0.2	1.7	1.9	0.2	0.0
18-49y	0.2	0.9	1.7	0.2	0.0
50-64y	0.2	0.7	1.2	1.0	0.1
65y+	0.1	0.7	1.0	0.3	0.6

Table A4.2 School contact matrix. Daily number contacts by age group at school.

	0-4y	**5-17y**	**18-49y**	**50-64y**	**65y+**
0-4y	1.0	0.5	0.4	0.1	0.0
5-17y	0.2	3.7	0.9	0.1	0.0
18-49y	0.0	0.7	0.8	0.0	0.0
50-64y	0.1	0.8	0.5	0.1	0.0
65y+	0.0	0.0	0.1	0.0	0.0

Table A4.3 Work contact matrix. Daily number contacts by age group at work.

	0-4y	**5-17y**	**18-49y**	**50-64y**	**65y+**
0-4y	0.0	0.0	0.0	0.0	0.0
5-17y	0.0	0.1	0.4	0.0	0.0
18-49y	0.0	0.2	4.5	0.8	0.0
50-64y	0.0	0.1	2.8	0.9	0.0
65y+	0.0	0.0	0.1	0.0	0.0

Table A4.4 Others contact matrix. Daily number contacts by age group at other locations.

	0-4y	5-17y	18-49y	50-64y	65y+
0-4y	0.7	0.7	1.8	0.6	0.3
5-17y	0.2	2.6	2.1	0.4	0.2
18-49y	0.1	0.7	3.3	0.6	0.2
50-64y	0.1	0.3	2.2	1.1	0.4
65y+	0.0	0.2	1.3	0.8	0.6

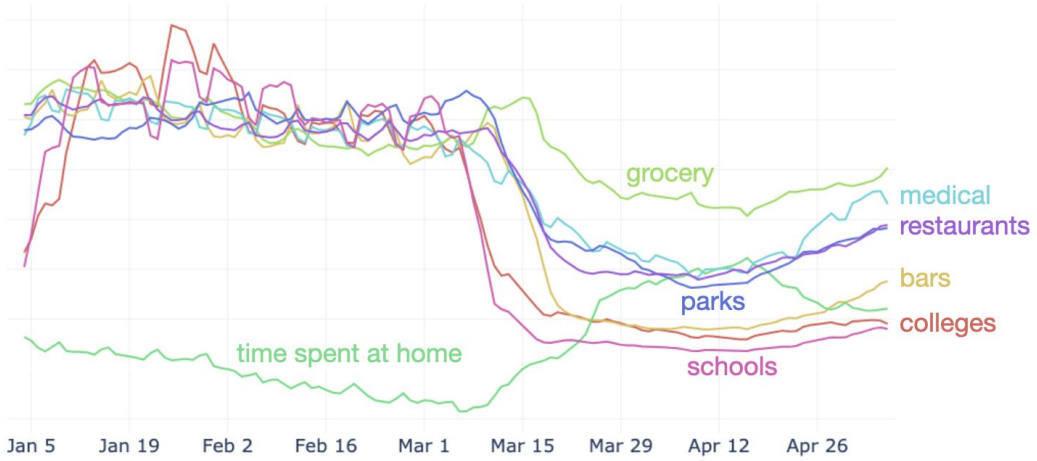

Figure A2. Mobility estimates for the Houston MSA based on SafeGraph cell phone geolocation traces [15]**.** Proportion of time spent at home (lower green line) begins to climb in early March, while daily number of visits to public points of interest, including college campuses (colleges), bars, restaurants, parks, schools, grocery stores, and healthcare providers (medical) decreases. We used these data for Houston, TX from January 4 - May 6 2020 to inform our estimates of the timing of reduced mobility.

Estimation of age-stratified proportion of population at high-risk for COVID-19 complications

We estimate age-specific proportions of the population at high risk of complications from COVID-19 based on data for Houston, TX from the CDC's 500 cities project (Figure A3) [16]. We assume that high risk conditions for COVID-19 are the same as those specified for influenza by the CDC [11]. The CDC's 500 cities project provides city-specific estimates of prevalence for several of these conditions among adults [17]. The estimates were obtained from the 2015-2016 Behavioral Risk Factor Surveillance System (BRFSS) data using a small-area estimation

methodology called multi-level regression and poststratification [12,13]. It links geocoded health surveys to high spatial resolution population demographic and socioeconomic data [13].

Estimating high-risk proportions for adults. To estimate the proportion of adults at high risk for complications, we use the CDC's 500 cities data, as well as data on the prevalence of HIV/AIDS, obesity and pregnancy among adults (Table A6).

The CDC 500 cities dataset includes the prevalence of each condition on its own, rather than the prevalence of multiple conditions (e.g., dyads or triads). Thus, we use separate co-morbidity estimates to determine overlap. Reference about chronic conditions [18] gives US estimates for the proportion of the adult population with 0, 1 or 2+ chronic conditions, per age group. Using this and the 500 cities data we can estimate the proportion of the population p_{HR} in each age group in each city with at least one chronic condition listed in the CDC 500 cities data (Table A6) putting them at high-risk for flu complications.

HIV: We use the data from table 20a in CDC HIV surveillance report [19] to estimate the population in each risk group living with HIV in the US (last column, 2015 data). Assuming independence between HIV and other chronic conditions, we increase the proportion of the population at high-risk for influenza to account for individuals with HIV but no other underlying conditions.

Morbid obesity: A BMI over 40kg/m^2 indicates morbid obesity, and is considered high risk for influenza. The 500 Cities Project reports the prevalence of obese people in each city with BMI over 30kg/m^2 (not necessarily morbid obesity). We use the data from table 1 in Sturm and Hattori [20] to estimate the proportion of people with BMI>30 that actually have BMI>40 (across the US); we then apply this to the 500 Cities obesity data to estimate the proportion of people who are morbidly obese in each city. Table 1 of Morgan et al. [21] suggests that 51.2% of morbidly obese adults have at least one other high risk chronic condition, and update our high-risk population estimates accordingly to account for overlap.

Pregnancy: We separately estimate the number of pregnant women in each age group and each city, following the methodology in CDC reproductive health report [22]. We assume independence between any of the high-risk factors and pregnancy, and further assume that half the population are women.

Estimating high-risk proportions for children. Since the 500 Cities Project only reports data for adults 18 years and older, we take a different approach to estimating the proportion of children at high risk for severe influenza. The two most prevalent risk factors for children are asthma and obesity; we also account for childhood diabetes, HIV and cancer.
From Miller et al. [23], we obtain national estimates of chronic conditions in children. For asthma, we assume that variation among cities will be similar for children and adults. Thus, we use the relative prevalences of asthma in adults to scale our estimates for children in each city. The prevalence of HIV and cancer in children are taken from CDC HIV surveillance report [19] and cancer research report [24], respectively.

We first estimate the proportion of children having either asthma, diabetes, cancer or HIV (assuming no overlap in these conditions). We estimate city-level morbid obesity in children using the estimated morbid obesity in adults multiplied by a national constant ratio for each age group estimated from Hales et al. [25], this ratio represents the prevalence in morbid obesity in children given the one observed in adults. From Morgan et al. [21], we estimate that 25% of morbidly obese children have another high-risk condition and adjust our final estimates accordingly.

Resulting estimates. We compare our estimates for the Houston Metropolitan Area to published national-level estimates [26] of the proportion of each age group with underlying high risk conditions (Table A6). The biggest difference is observed in older adults, with Houston having a lower proportion at risk for complications for COVID-19 than the national average; for 25-39 year olds the high risk proportion is slightly higher than the national average.

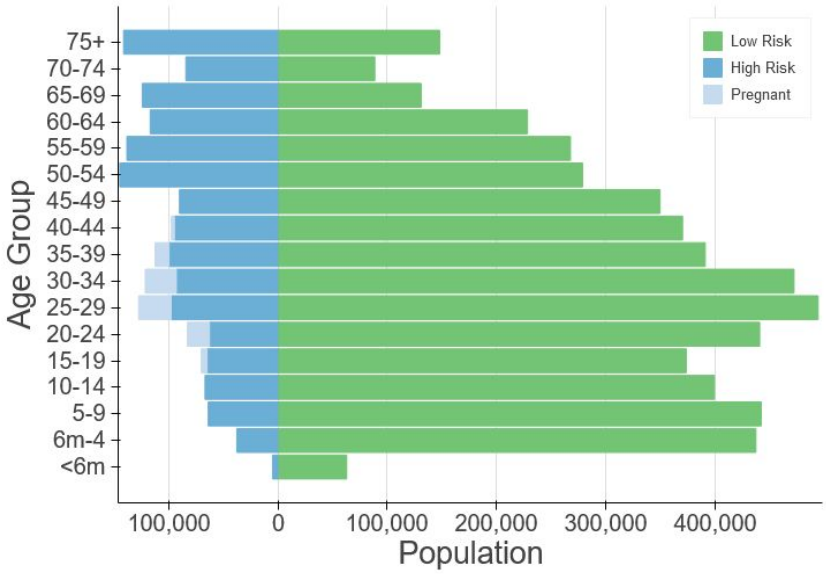

Figure A3. Demographic and risk composition of the Houston MSA. Bars indicate age-specific population sizes, separated by low risk, high risk, and pregnant. High risk is defined as individuals with cancer, chronic kidney disease, COPD, heart disease, stroke, asthma, diabetes, HIV/AIDS, and morbid obesity, as estimated from the CDC 500 Cities Project [16] reported HIV prevalence [19] and reported morbid obesity prevalence [20,21] corrected for multiple conditions. The population of pregnant women is derived using the CDC's method combining fertility, abortion and fetal loss rates [27–29].

Table A6. High-risk conditions for influenza and data sources for prevalence estimation

Condition	Data source
Cancer (except skin), chronic kidney disease, COPD, coronary heart disease, stroke, asthma, diabetes	CDC 500 cities [16]
HIV/AIDS	CDC HIV Surveillance report [19]
Obesity	CDC 500 cities [16], Sturm and Hattori [20], Morgan et al.[21]
Pregnancy	National Vital Statistics Reports [27] and abortion data [28]

Table A7: Comparison between published national estimates and Houston MSA estimates of the percent of the population at high-risk of influenza/COVID-19 complications.

Age Group	National estimates [25]	Houston (excluding pregnancy)	Pregnant women (proportion of age group)
0 to 6 months	NA	6.8	-
6 months to 4 years	6.8	7.4	-
5 to 9 years	11.7	11.6	-
10 to 14 years	11.7	13.0	-
15 to 19 years	11.8	13.3	1.7
20 to 24 years	12.4	10.3	5.1
25 to 34 years	15.7	13.5	7.8
35 to 39 years	15.7	17.0	5.1
40 to 44 years	15.7	17.4	1.2
45 to 49 years	15.7	17.7	-
50 to 54 years	30.6	29.6	-
55 to 60 years	30.6	29.5	-
60 to 64 years	30.6	29.3	-
65 to 69 years	47.0	42.2	-
70 to 74 years	47.0	42.2	-
75 years and older	47.0	42.2	-

References

1. Keeling MJ, Rohani P. Modeling Infectious Diseases in Humans and Animals. Princeton University Press; 2011. Available: https://play.google.com/store/books/details?id=LxzILSuKDhUC

2. Gillespie DT. Approximate accelerated stochastic simulation of chemically reacting systems. J Chem Phys. 2001;115: 1716–1733. doi:10.1063/1.1378322

3. Halfin S, Whitt W. Heavy-Traffic Limits for Queues with Many Exponential Servers. Oper Res. 1981;29: 567–588. doi:10.1287/opre.29.3.567

4. Duque D, Morton DP, Singh B, Du Z, Pasco R, Meyers LA. COVID-19: How to Relax Social Distancing If You Must. medRxiv. 2020. Available: https://www.medrxiv.org/content/10.1101/2020.04.29.20085134v1.abstract

5. minimize(method='trust-constr') — SciPy v1.4.1 Reference Guide. [cited 19 Apr 2020]. Available: https://docs.scipy.org/doc/scipy/reference/optimize.minimize-trustconstr.html

6. He X, Lau EHY, Wu P, Deng X, Wang J, Hao X, et al. Temporal dynamics in viral shedding and transmissibility of COVID-19. Nat Med. 2020. doi:10.1038/s41591-020-0869-5

7. Gudbjartsson DF, Helgason A, Jonsson H, Magnusson OT, Melsted P, Norddahl GL, et al. Spread of SARS-CoV-2 in the Icelandic Population. N Engl J Med. 2020. doi:10.1056/NEJMoa2006100

8. Zhang J, Litvinova M, Wang W, Wang Y, Deng X, Chen X, et al. Evolving epidemiology and transmission dynamics of coronavirus disease 2019 outside Hubei province, China: a descriptive and modelling study. Lancet Infect Dis. 2020. doi:10.1016/S1473-3099(20)30230-9

9. He D, Zhao S, Lin Q, Zhuang Z, Cao P, Wang MH, et al. The relative transmissibility of asymptomatic COVID-19 infections among close contacts. Int J Infect Dis. 2020;94: 145–147. doi:10.1016/j.ijid.2020.04.034

10. Verity R, Okell LC, Dorigatti I, Winskill P, Whittaker C, Imai N, et al. Estimates of the severity of COVID-19 disease. Epidemiology. medRxiv; 2020. doi:10.1101/2020.03.09.20033357

11. CDC. People at High Risk of Flu. In: Centers for Disease Control and Prevention [Internet]. 1 Nov 2019 [cited 26 Mar 2020]. Available:

https://www.cdc.gov/flu/highrisk/index.htm

12. CDC - BRFSS. 5 Nov 2019 [cited 26 Mar 2020]. Available: https://www.cdc.gov/brfss/index.html

13. Zhang X, Holt JB, Lu H, Wheaton AG, Ford ES, Greenlund KJ, et al. Multilevel regression and poststratification for small-area estimation of population health outcomes: a case study of chronic obstructive pulmonary disease prevalence using the behavioral risk factor surveillance system. Am J Epidemiol. 2014;179: 1025–1033. doi:10.1093/aje/kwu018

14. Tindale L, Coombe M, Stockdale JE, Garlock E, Lau WYV, Saraswat M, et al. Transmission interval estimates suggest pre-symptomatic spread of COVID-19. Epidemiology. medRxiv; 2020. doi:10.1101/2020.03.03.20029983

15. SafeGraph | POI Data, Business Listings, & Foot-Traffic Data. [cited 17 Apr 2020]. Available: https://www.safegraph.com/

16. 500 Cities Project: Local data for better health | Home page | CDC. 5 Dec 2019 [cited 19 Mar 2020]. Available: https://www.cdc.gov/500cities/index.htm

17. Health Outcomes | 500 Cities. 25 Apr 2019 [cited 28 Mar 2020]. Available: https://www.cdc.gov/500cities/definitions/health-outcomes.htm

18. Part One: Who Lives with Chronic Conditions. In: Pew Research Center: Internet, Science & Tech [Internet]. 26 Nov 2013 [cited 23 Nov 2019]. Available: https://www.pewresearch.org/internet/2013/11/26/part-one-who-lives-with-chronic-conditions/

19. for Disease Control C, Prevention, Others. HIV surveillance report. 2016; 28. URL: http://www cdc gov/hiv/library/reports/hiv-surveil-lance html Published November. 2017.

20. Sturm R, Hattori A. Morbid obesity rates continue to rise rapidly in the United States. Int J Obes . 2013;37: 889–891. doi:10.1038/ijo.2012.159

21. Morgan OW, Bramley A, Fowlkes A, Freedman DS, Taylor TH, Gargiullo P, et al. Morbid obesity as a risk factor for hospitalization and death due to 2009 pandemic influenza A(H1N1) disease. PLoS One. 2010;5: e9694. doi:10.1371/journal.pone.0009694

22. Estimating the Number of Pregnant Women in a Geographic Area from CDC Division of Reproductive Health. Available: https://www.cdc.gov/reproductivehealth/emergency/pdfs/PregnacyEstimatoBrochure508.pdf

23. Miller GF, Coffield E, Leroy Z, Wallin R. Prevalence and Costs of Five Chronic

Conditions in Children. J Sch Nurs. 2016;32: 357–364. doi:10.1177/1059840516641190

24. Cancer Facts & Figures 2014. [cited 30 Mar 2020]. Available: https://www.cancer.org/research/cancer-facts-statistics/all-cancer-facts-figures/cancer-facts-figures-2014.html

25. Hales CM, Fryar CD, Carroll MD, Freedman DS, Ogden CL. Trends in Obesity and Severe Obesity Prevalence in US Youth and Adults by Sex and Age, 2007-2008 to 2015-2016. JAMA. 2018;319: 1723–1725. doi:10.1001/jama.2018.3060

26. Zimmerman RK, Lauderdale DS, Tan SM, Wagener DK. Prevalence of high-risk indications for influenza vaccine varies by age, race, and income. Vaccine. 2010;28: 6470–6477. doi:10.1016/j.vaccine.2010.07.037

27. Martin JA, Hamilton BE, Osterman MJK, Driscoll AK, Drake P. Births: Final Data for 2017. Natl Vital Stat Rep. 2018;67: 1–50. Available: https://www.ncbi.nlm.nih.gov/pubmed/30707672

28. Jatlaoui TC, Boutot ME, Mandel MG, Whiteman MK, Ti A, Petersen E, et al. Abortion Surveillance - United States, 2015. MMWR Surveill Summ. 2018;67: 1–45. doi:10.15585/mmwr.ss6713a1

29. Ventura SJ, Curtin SC, Abma JC, Henshaw SK. Estimated pregnancy rates and rates of pregnancy outcomes for the United States, 1990-2008. Natl Vital Stat Rep. 2012;60: 1–21. Available: https://www.ncbi.nlm.nih.gov/pubmed/22970648